Magnesium Impregnated Silica Mesoporous Prepared using Ester Ricinoleic as Template for the Esterification

Andriayani[1,2*], Marpongahtun[1], Yugia Muis[1]
[1]*Department of Chemistry, Faculty of Mathematics and Natural Science, Universitas Sumatera Utara, Medan, Indonesia, 20155*
[2]*Pusat Kajian IPTEKS Minyak Atsiri Eucaplytus Universitas Sumatera Utara, Medan, 20155, Indonesia*

Keywords: mesoporous silica, ester ricinoleic, template, magnesium.

Abstract: Synthesis of mesoporous silica material was carried out using ricinoleate ester as a template. Mesoporous silica products were characterized using FT-IR, XRD, SEM and nitrogen adsorption. Mesoporous silica material was impregnated with magnesium nitrate, impregnation products were characterized using FT-IR, XRD, SEM and BET analysis. MgO impregnated silica mesoporous is applied as a catalyst in the reaction of esterification of castor oil to ricinoleate ester.

1 INTRODUCTION

Porosity greatly influences the physical properties of a material such as density, heat conductivity, strength and others (Schubert, Ulrich S. and Husing, 2005). The synthesis technique of mesopore material (2-50 nm pore diameter) is currently developing rapidly because mesopore material has unique properties, such as a more regular pore structure, large surface area and uniform pore size distribution. So much applied as catalysts (Li *et al.*, 2011), adsorbents (Yan *et al.*, 2006), drug delivery (Slowing *et al.*, 2008), biosensors (Hasanzadeh *et al.*, 2012), optics (Kumari and Sahare, 2013) and others.

The synthesis technique of mesoporous material is carried out by combining inorganic components as material and organic components such as surfactants functioning as pore printers (templates). The pore will be obtained after the organic component has been removed by calcination.

In this paper, tetraethylortosilicate (TEOS) is used as a source of silica, risinolet methyl ester as a template is made by extracting Ricinus communis seeds that grow in wild forests in the North Sumatera Karo region. Also used are 3-aminopropyltrimethoxysilane (APMS) as a co-structure directing agent (CSDA). The alkoxylane group from CSDA will condense with inorganic precursors and the ammonium group will interact electrostatically with anionic surfactants. The interaction that occurs between surfactant and silicate is S-N^+ I^- where N^+ is CSDA.

In the previous study (Andriayani *et al.*, 2013) have been done synthesized of material silica using sodium risinoleate as a template by varying the addition of HCl 0,1N. In this paper we impregnate MgO on silica mesoporous which is made using methyl ester ricinoleate as a template and analyzed using FT-IR, XRD, SEM and BET. The mesoporous silica impregnation product was applied as a catalyst in the reaction of castor oil eseterification to ricinoleate ester. Given the increasingly limited fossil fuels, ricinoleic esters can be an alternative to fuels sourced from plants.

2 MATERIALS AND METHODS

2.1 Materials

Tetraethylorthosilicate (TEOS, 98%) and 3-aminopropyltrimethoxysilane (APMS) were purchased from Sigma Aldrich, methanol, and hexane purcase from Emerc, methyl esther ricinoleic acid ($C_{19}H_{36}O_3$) obtained from Ricinus Communis seed and deionized water obtained from PT Sumber Aneka Karya Abadi. Jatropha seed oil is obtained from Bratachem, $Mg(NO_3)_2$ (Merck), n-hexene.

Andriayani, ., Marpongahtun, . and Muis, Y.
Magnesium Impregnated Silica Mesoporous Prepared using Ester Ricinoleic as Template for the Esterification.
DOI: 10.5220/0008921702740279
In *Proceedings of the 1st International Conference on Chemical Science and Technology Innovation (ICOCSTI 2019)*, pages 274-279
ISBN: 978-989-758-415-2

2.2 Characterizations

The obtained products were then subjected to characterization by using X-ray diffraction (Philip PW 1710), Fourier transform infrared (Shimadzu IR-Prestige-21), scanning electron microscope (JEOL JSM-7000F), transmission electron microscope (JEOL JEM-1400) and adsorption desorption isotherm (Quantachrome Auto¬sorb), Atomic absorption spectroscopy (Shimadzu AA7000).

2.3 Synthesis of Silica Mesoporous Material using Risinoleic Methyl Ester as a Template

Methyl esters of ricinoleate ($C_{19}H_{36}O_3$) of 4.52 g (0.015 mol), 100 ml deionized water and 1.2 grams of methanol were put into two neck flasks and sterilized at room temperature for 30 minutes (mix A). Then a mixture of 1.2 g (0.007 mol) APMS ($C_6H_{17}SiO_3N$) and 6.04 g (0.029 mol) TEOS (C_8H_{20} SiO_4) was stirred for 10 minutes (mixture B).

The mixture (B) was added to the mixture (A) and then stirred for 2 hours. Then let it sit in the oven at 80ºC for 3 days (36 hours) until a porous solid is formed. The mixture is centrifuged and the solids are separated and washed with deionized water. The solid is dried at 50□C and then calcined at 550□C for 6 hours. Silica mesoporous products were then characterized using FT-IR, XRD, SEM analysis and N_2 isotherm adsorption / desorption.

2.4 Impregnation of Mesoporous Silica Material with Magnesium

Silica mesoporous material (0.75 gram) mixed with $Mg(NO_3)_2.6H_2O$ (g) and added 25 mL of dry methanol, then stirred at room temperature for 2 hours. The mixture is vacuumed to dry solids and then solids are calcined for 12 hours at 550ºC. Mesoporous silica impregnation products were characterization using FT-IR, XRD, AAS, BET and SEM.

2.5 Application of Mesoporous Silica Impregnation Products as Esterification Catalyst

Mesoporous silica impregnation products (0.2 g), methanol (p.a) (6.14 g) and castor oil (15 grams) were put into a two neck flask. The mixture is stirred with a magnetic stirrer for 4 hours at 80° C by reflux method. The solid is separated from the reaction mixture by filtering. The filtrate is extracted using n-hexane and distilled water. Then the n-hexane phase was vacuum and a pale yellow methyl ester product of 10.59 grams or 70.6% yield was obtained. The ricinoleate methyl ester product was characterized using FT-IR and GC-MS.

3 RESULTS AND DISCUSSION

The silica mesoporous used to be applied as a catalyst was obtained from one of the silica mesoporous under the conditions of the preparation of methanol addition variations without the addition of 0.1M HCl. The reaction conditions for mesoporous silica preparation using tetraethylortosilicate (TEOS) as a source of silica, methyl ester risinoleate obtained from esterification of castor oil from castor beans (Ricinus communis) as a template, using 3-aminopropiltrimethoxysilane (APMS) as a co-structure directing agent and adding methanol 1 2 grams without the addition of 0.1M HCl. After maturing for 72 hours, the solid is separated, washed, dried and to remove the template calcined at 550ºC for 6 hours a white solid is obtained. Furthermore, it is characterized by FT-IR, XRD, SEM and porosity analysis using BET.

Mesoporous silica is impregnated using $Mg(NO_3)_2$ in a dry methanol solvent, the solid is separated, vacuum and calcined at 550ºC for 12 hours. White solids were obtained as much as 0.6415 grams. Mesoporous silica impregnation with Mg $(NO_3)_2$ produced silica-MgO mesoporous (MS-MgO). Magnesium oxide is attached to the surface of the mesoporous silica material. AAS analysis results showed that the Mg content contained in mesoporous silica material was 1.3549 ppm. Subsequently the solids were characterized using FT-IR, XRD, SEM and porosity analysis using BET.

Functional group analysis using the FT-IR spectrum of mesoporous silica that has not been impregnated with silica mesoporous that has been impregnated with MgO (Figure 1) shows the change in functional groups in both materials. The mesoporous silica spectrum before impregnation (Figure 7 in black) showed an absorption peak at 3428.58 cm^{-1} which was widening due to OH (strain Si-OH) strain and supported the absorption peak at 964.41 cm^{-1} due to streching (–SiO-H). The absorption peak at 1103.28 cm^{-1} is strong due to the asymmetric streching of Si-O-Si and the wave number at 810.10 cm^{-1} is caused by the presence of symmetrical Si-O-Si. The spectrum data is adjusted to the literature: (Khalil, 2007; AlOthman and Apblett, 2010; Liu *et al.*, 2010; Zhao *et al.*, 2011). While the mesoporous silica spectrum that has been impregnated by MgO shows the absorption peak at 3448.72 cm^{-1} which was widened due to OH group

strain (Si-OH) and supported the absorption peak at 887.26 cm^{-1} due to streching (–SiO-H). The absorption peak at 1103.28 cm^{-1} is strong due to the asymmetric streching of Si-O-Si and the wave number at 810.10 cm^{-1} is caused by the presence of symmetrical Si-O-Si groups.

The peak absorption of Si-OH groups is different compared to mesoporous silica before being impregnated where the peak shape is not too wide and there is a shift in the wave number. This is due to the surface of the silanol group which has been impregnated with MgO. Likewise with the peak caused by the Si-O-Si group there is a difference compared to the mesoporous before digrafting such as a sharp peak shape but not widening (slimmer) with an intensity of 5.19 while for the mesoporous silica the sharp peak shape widens and the intensity is low 0.04. This is due to the mesoporous that has been impregnated by the formation of Si-O-M bonds (M = metal Mg) which is in the wave number 1000-900 with a strong band (Smith, 1960).

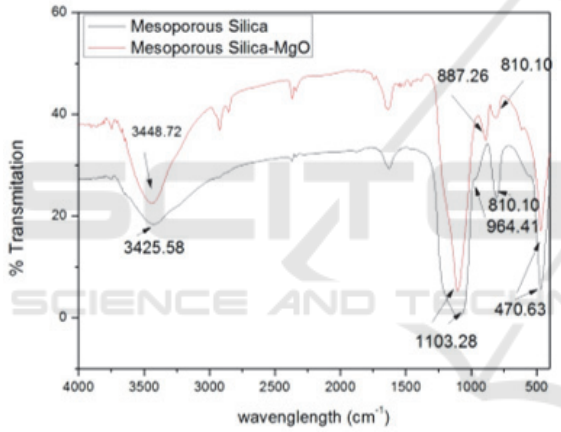

Figure 1: Mesoporous Silica FT-IR Spectrum Before Impregnation and After MgO Impregnation

Analysis of the mesoporous silica structure before impregnation and after impregnation (Figure 2) shows the differences in the diffractogram of the two materials. The mesoporous XRD diffractogram of silica before impregnation (Figure 2 in black) has only one diffractogram peak at an angle of 2θ at 20.9865° the broad peak (broad) with a peak height of 14.20. This shows that the material is nanoparticles and amorphous structures that have pores. This is consistent with data reported by previous researchers (Park *et al.*, 2006; Khalil, 2007; Shah, Li and Ali Abdalla, 2009; Liu *et al.*, 2010; 'No Title', 2011; Li *et al.*, 2011; Zhao *et al.*, 2011).

Whereas the mesoporous silica diffractogram that has been impregnated with MgO (Figure 2 in red) has several diffractogram peaks. Diffractogram at an angle of 2θ at 22.8454° with a peak that widened to a height of 31.63 indicates that the material is nanoparticles with a porous amorphous structure. Whereas the diffractogram at 2θ at 32°, 35°, 36°, 39°, 42° and 45° is the peak of the Mg metal diffractogram which is impregnated on the silica mesoporous surface. This proves the process of mesoporous silica impregnation has taken place.

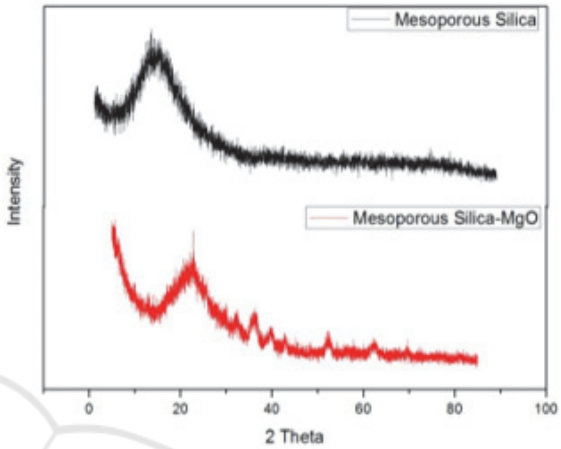

Figure 2: XRD Diffractogram of Mesoporous Silica Mesopori Before Impregnation and After MgO Impregnation

Mesoporous morphological analysis of the silica before impregnation (Figure 3) using a scanning electron microscope (SEM) magnification 15000 times and 20000 times showed that the material has a mixed particle form, dominated by dispersed spherical particles and some that form smaller aggregates. Other particles in the form of sheets with a small amount.

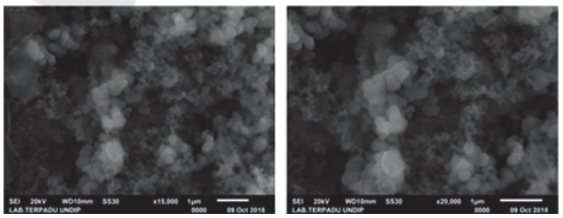

Figure 3: SEM Image of Mesoporous Silica Before MgO Impregnation (left 15000 times and right 20000 times magnification)

Analysis of porosity of silica material before impregnation and after impregnation of MgO (Figure 5) shows the differences in adsorption desorption isotherm graphs. Based on its hysterical form, silica material approaches Type IV for silica mesoporous according to the specific IUPAC classification for silica mesoporous material. Graph

of silica meopore desorption adsorption before impregnation (Figure 5 in black) lop hysteresis form is Type H4, where the lop's hysteresis form is a bit more complex because of the reversible micropore filling area followed by multilayer physisorption and capillary condensation. So lop H4 is the same as lop H3 for non-micropore materials.

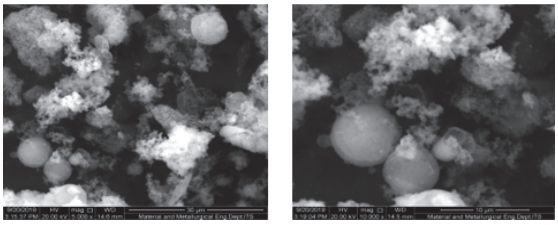

Figure 4: SEM Image of Mesoporous Silica After MgO Impregnation (left 15000 times and right 20000 times magnification)

While the graph of adsorption desorption isotherm of silica mesoporous material after MgO impregnation (Figure 5 in red) the form of hysteresis is Type H3 (Sing and Williams, 2004). This is due to the shape of aggregate and plate particles, characteristic desorption grooves and lower approaching end points (closure points). Lop H3 does not have a plateau at high P/P0 values (mesoporous volume is not well formulated), so interpretation of high P/P0 values is more difficult. Branch adsorption graphs on type H3 show that gas adsorption only occurs on surfaces or manolayers so that this shows that the obtained silica material can be grouped also on Type II isotherm charts for non-porous solids (Gregg S. J., and Sing, 1982). This is due to the silica impregnated surface of MgO in the pores that are already covered by MgO so that the shape of the hysteresis loop resembles non-pore solids.

Graph of mesoporous silica pore size distribution before impregnation and silica mesoporous after pregreated MgO (Figure 6) were calculated using the Barret-Joyner-Halenda (BJH) method. The pore size distribution of the two materials shows a difference. The mesopore pore size distribution before impregnation (Figure 5 in black) shows the pore size distribution in the range of 1.64 nm - 8.105 nm. While the pore size distribution of silica mesoporous material that has been impregnated by MgO shows that the pore size distribution is in the range of 1.61 nm - 9.31 nm.

The pore size distribution graph of the two materials has a difference in the dV / dD value, which is because there is a re-calcination treatment for silica mesoporous MgO impregnated causing the number of pores formed in the range of pore size distribution of 1 nm - 6 nm to increase. Whereas the dV/dD value of mesoporous material before impregnation with the same (smaller) pore size distribution range. But the dV/dD value in the pore size distribution from 6-10 nm for mesoporous materials impregnated with MgO is getting smaller because the pores are covered with MgO, whereas the silica mesoporous material before the impregnation of dV/dD values in the same pore size distribution range is smaller big because it's not covered in metal.

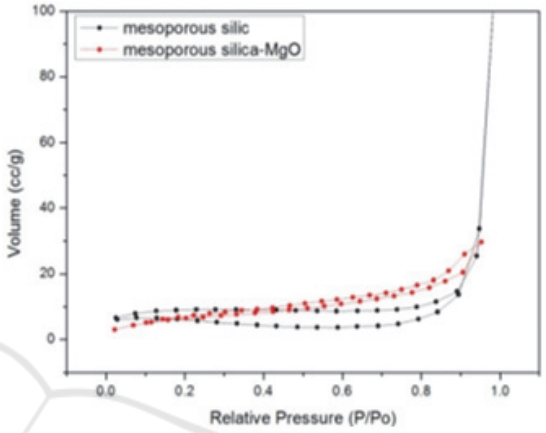

Figure 5: Adsorption Graph Desorption of Silica Mesoporous Isotherm Before Impregnation and After MgO Impregnation

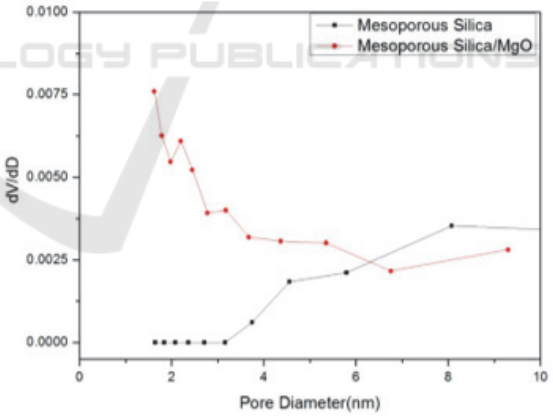

Figure 6: Graphs of Silica Mesoporous Pore Size Distribution Before Imprgenation and After MgO Impregnation

The silica mesoporous material impregnated by MgO was tested for its catalytic activity in the esterification reaction of castor oil. The catalytic system of esterification reaction takes place under heterogeneous conditions where mesoporous silica-MgO is insoluble (remains solid). Such reaction conditions are advantageous because they are easily separated between the product and the catalyst. The

reaction was carried out at 80°C for 4 hours. After the reaction is stopped, the catalyst solids are separated and the filtrate is extracted with n-hexane and washed with distilled water, after vacuum the product has obtained a pale yellow methyl ester product of 10.59 grams or a yield of 70.6%. The ricinoleate methyl ester product was characterized using FT-IR and GC-MS.

The formation of ricinoleate methyl ester product was characterized using FT-IR and GC-MS. FT-IR spectrum of methyl ester ricinoleate castor oil esterification product (castor oil) using silica-MgO mesoporous catalyst (Figure 7) shows the appearance of widening at 3417.86 cm^{-1} due to OH groups in the carbon chain of methyl ester ester risinoleate. While the sharp peak at 2854.65 cm^{-1} is caused by the vibration frequency of the -CH- hydrocarbon chain group of methyl ester ricinoleate. Another sharp peak at 1743.65 cm^{-1} was caused by the carbonyl methyl ester ricinoleate group.

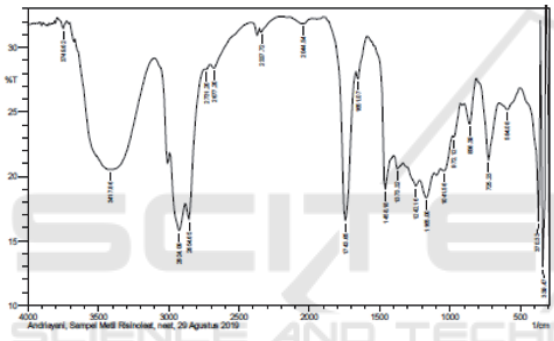

Figure 7: FT-IR Spectra of Risinoleate FT-IR Spectrum

Transeterification of castor oil using mesoporous silica-MgO-catalyzed methanol produces a mixture of fatty acid methyl esters. This is due to the distance that there are other fatty acids such as ricinoleic acid, palmitic acid, stearic acid, linoleic acid, oleic acid and others. So if esterified other fatty acids might also be esterified. To find out the composition of methyl esters formed from castor oil, GC-MS analysis was performed. Through GC-MS method, it can be known the percentage of methyl esters of ricinoleate formed through the application of silica-MgO mesoporous catalyst. The results of GC-MS chromatogram of castor oil esterification products with a heterogeneous reaction system (Figure 8) can be seen that the risinoleate methyl ester formed has a remaining 84.48% purity of 15.52% is a methyl ester from other fatty acids.

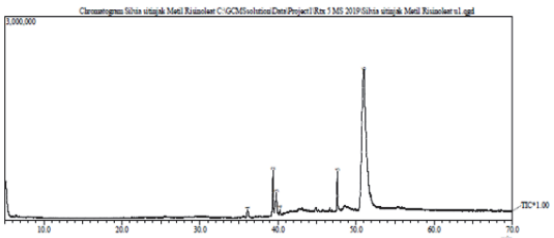

Figure 8: Chromatogram GC-MS of Risinoleate Esther

4 CONCLUSIONS

The mesoporous silica impregnation which was made using methyl ester ricinoleate as a template was successfully carried out. This can be proven by the differences in analysis of mesoporous silica products before being impregnated and after being impregnated, it can be proven from FT-IR, XRD and BET analysis. Its application as a catalyst in castor oil esterification reaction results in ricinoleate ester of 10.96 g (73.06%).

ACKNOWLEDGEMENTS

This research was funded by the DRPM Republic of Indonesia Ministry of Research and Technology Republic of Indonesia Fiscal Year 2019.

REFERENCES

AlOthman, Z. A. and Apblett, A. W. (2010) 'Synthesis and characterization of a hexagonal mesoporous silica with enhanced thermal and hydrothermal stabilities', *Applied Surface Science*, 256(11), pp. 3573–3580. doi: 10.1016/j.apsusc.2009.12.157.

Andriayani, A. *et al.* (2013) 'Synthesis of Mesoporous Silica from Tetraethylorthosilicate by Using Sodium Ricinoleic as a Template and 3-Aminopropyltrimethoxysilane as Co-Structure Directing Agent with Volume Variation of Hydrochloric Acid 0.1 M', *Advanced Materials Research*, 789, pp. 124–131. doi: 10.4028/www.scientific.net/AMR.789.124.

Gregg S. J., and Sing, K. S. W. (1982) *Adsorpsi, Surface Area and Porosity*. Second Edi. London: Academic Press.

Hasanzadeh, M. *et al.* (2012) 'Mesoporous silica-based materials for use in biosensors', *TrAC* -

Trends in Analytical Chemistry, 33, pp. 117–129. doi: 10.1016/j.trac.2011.10.011.

Khalil, K. M. S. (2007) 'Cerium modified MCM-41 nanocomposite materials via a nonhydrothermal direct method at room temperature', *Journal of Colloid and Interface Science*, 315(2), pp. 562–568. doi: 10.1016/j.jcis.2007.07.030.

Kumari, S. and Sahare, P. D. (2013) 'Optical studies of fluorescent mesoporous silica nanoparticles', *Journal of Materials Science and Technology*. Elsevier Ltd, 29(8), pp. 742–746. doi: 10.1016/j.jmst.2013.05.013.

Li, B. *et al.* (2011) 'Preparation of MCM-41 incorporated with transition metal substituted polyoxometalate and its catalytic performance in esterification', *Microporous and Mesoporous Materials*. Elsevier Inc., 156(1), pp. 73–79. doi: 10.1016/j.micromeso.2012.02.017.

Liu, H. *et al.* (2010) 'Synthesis of spherical-like Pt-MCM-41 meso-materials with high catalytic performance for hydrogenation of nitrobenzene', *Journal of Colloid and Interface Science*. Elsevier Inc., 346(2), pp. 486–493. doi: 10.1016/j.jcis.2010.03.018.

'No Title' (2011), 08(03), pp. 71–79.

Park, Y. *et al.* (2006) 'Encapsulation method for the dispersion of NiO onto ordered mesoporous silica, SBA-15, using polyethylene oxide (PEO)', *Journal of Colloid and Interface Science*, 295(2), pp. 464–471. doi: 10.1016/j.jcis.2005.09.006.

Schubert, Ulrich S. and Husing, N. (2005) *Synthesis of Inorganic Materials*. 2nd, Revis edn. German: Wiley-VCH.

Shah, A. T., Li, B. and Ali Abdalla, Z. E. (2009) 'Direct synthesis of Ti-containing SBA-16-type mesoporous material by the evaporation-induced self-assembly method and its catalytic performance for oxidative desulfurization', *Journal of Colloid and Interface Science*. Elsevier Inc., 336(2), pp. 707–711. doi: 10.1016/j.jcis.2009.04.026.

Slowing, I. I. *et al.* (2008) 'Mesoporous silica nanoparticles as controlled release drug delivery and gene transfection carriers', *Advanced Drug Delivery Reviews*, 60(11), pp. 1278–1288. doi: 10.1016/j.addr.2008.03.012.

Smith, A. L. (1960) 'Infrared spectra-structure correlations for organosilicon compounds', *Spectrochimica Acta*, 16(1–2), pp. 87–105. doi: 10.1016/0371-1951(60)80074-4.

Yan, Z. *et al.* (2006) 'Pyridine-functionalized mesoporous silica as an efficient adsorbent for the removal of acid dyestuffs', *Journal of Materials Chemistry*, 16(18), pp. 1717–1725. doi: 10.1039/b517017f.

Zhao, Q. *et al.* (2011) 'Stability and textural properties of cobalt incorporated MCM-48 mesoporous molecular sieve', *Applied Surface Science*. Elsevier B.V., 257(7), pp. 2436–2442. doi: 10.1016/j.apsusc.2010.09.114.